

Band gap states of copper phthalocyanine thin films induced by nitrogen exposure

Tomoki Sueyoshi, Haruya Kakuta, Masaki Ono, Kazuyuki Sakamoto, Satoshi Kera et al.

Citation: *Appl. Phys. Lett.* **96**, 093303 (2010); doi: 10.1063/1.3332577

View online: <http://dx.doi.org/10.1063/1.3332577>

View Table of Contents: <http://apl.aip.org/resource/1/APPLAB/v96/i9>

Published by the [American Institute of Physics](http://www.aip.org).

Additional information on *Appl. Phys. Lett.*

Journal Homepage: <http://apl.aip.org/>

Journal Information: http://apl.aip.org/about/about_the_journal

Top downloads: http://apl.aip.org/features/most_downloaded

Information for Authors: <http://apl.aip.org/authors>

ADVERTISEMENT



Goodfellow
metals • ceramics • polymers • composites
70,000 products
450 different materials
small quantities fast

www.goodfellowusa.com

Band gap states of copper phthalocyanine thin films induced by nitrogen exposure

Tomoki Sueyoshi,^{a)} Haruya Kakuta, Masaki Ono, Kazuyuki Sakamoto, Satoshi Kera, and Nobuo Ueno

Graduate School of Advanced Integration Science, Chiba University, Yayoi-cho, Inage-ku, Chiba 263-8522, Japan

(Received 21 November 2009; accepted 4 February 2010; published online 3 March 2010)

The impact of 1 atm N₂ gas exposure on the electronic states of copper phthalocyanine thin films was investigated using ultrahigh-sensitivity ultraviolet photoelectron spectroscopy. The highest occupied molecular orbital band of the film showed a drastic reversible change in the bandwidth and band shape as well as in the energy position upon repeated cycles of N₂ exposure and subsequent annealing. Furthermore, two types of gap-state densities with Gaussian and exponential distributions appeared after the exposure and disappeared due to the annealing. These changes are ascribed to a weak disorder in the molecular packing structure induced by N₂ diffusion into the film. © 2010 American Institute of Physics. [doi:10.1063/1.3332577]

The mechanisms of the energy level alignment (ELA) of organic semiconductor interfaces have been investigated extensively to understand the fundamental physics of organic-conductor and organic-organic interfaces and to improve the performance of organic devices.¹⁻⁵ These studies have mainly focused on the energetic aspect of organic-based interface systems and thus on measurements of the energy difference between the highest occupied molecular orbital (HOMO), and the Fermi level of the substrate (E_F^S) and the vacuum level (VL) with ultraviolet photoelectron spectroscopy (UPS). Despite careful measurements of the interface electronic structure, the ELA mechanisms are still not comprehensively understood.^{2,3,5-7} The ELA mechanisms have been considered to originate in the undetectable density of gap states (DOGS) that controls the position of the HOMO relative to the Fermi level.⁵⁻⁸ A direct detection of very low-density band-gap states with UPS was reported recently for undoped pentacene ultrathin films, where the ELA was demonstrated to be controlled by such band gap states originating from an imperfect molecular packing structure at the interface.⁸

The exposure of organic-semiconductor films to gas atmospheres, such as oxygen, water vapor, and air, has also been reported to influence the ELA and electrical properties of organic devices.⁹⁻¹² The gas-exposure effects have been discussed in relation to chemical reactions or electron transfers between organic molecules and gas molecules.⁹⁻¹³ However, there is little discussion on the physical effects of the gas exposure on the electronic structure of organic thin films that consist of weakly interacting molecules with relatively large intermolecular spaces. Kondo *et al.*¹⁴ reported a large increase in the lattice parameters of a Cu(BF₄)₂(bpy)₂ (bpy = 4,4'-bipyridine) crystal upon CO₂ adsorption, where the increase was initiated by the penetration of gas molecules into the crystal depending on the gas pressure, size of nano-spaces in the crystal, and the chemical properties of the gas and crystal. This study suggests that an alteration of the molecular packing structure of an organic film may occur upon exposure to gas even when nonreactive gas is used. Such an

alternation influences the electronic structure of the films since (1) the gas penetration processes may introduce weak disorder in the molecular packing structure due to weak intermolecular interaction and (2) the valence band structure of organic solids has a sensitive dependency on the intermolecular packing geometry due to the low symmetry of the molecular structure.¹⁵ We investigated the effect of gas exposure on the electronic structure of organic thin films with UPS in order to examine the physical effects on organic devices under a 1 atm pressure condition.

Here, we report the impact of exposure to 1 atm N₂ on the electronic structure of a copper phthalocyanine (CuPc) thin film. The phenomena reported here were not observed for films exposed to lower-pressure N₂ gas. The HOMO band of the CuPc shifted toward the E_F^S , coupled with serious HOMO-band broadening and the appearance of band-gap states upon heavy N₂ exposure. The HOMO-band shift resembled that induced by *p*-type doping.

CuPc crystals purified by three cycles of vacuum sublimation were evaporated onto an Au substrate at 300 K at $<1 \times 10^{-7}$ Pa in the preparation chamber of a high-precision UPS system with ultrahigh sensitivity.⁸ The Au substrate was also prepared by vacuum deposition of Au on H-Si(111) in the preparation chamber. The deposition rate of CuPc was 0.1 nm/min as monitored by a quartz microbalance. The 7-nm-thick CuPc film was preannealed, exposed to 1 atm N₂ with a purity of 99.999 95% (6N5) at 300 K for 19 h using an ultrahigh vacuum (UHV)-compatible gas-inlet line mounted in the preparation chamber, and then postannealed at 343 K for more than 12 h at 4×10^{-8} Pa. UPS measurements were *in situ* repeated at 300 K before and after each annealing/N₂-exposure cycle by using the UPS apparatus with a monochromatic He I_α radiation ($h\nu=21.218$ eV) source described elsewhere.¹⁶ The energy resolution of the UPS system was set at 20 meV. All spectra were measured at normal emission with the acceptance angle of $\pm 7^\circ$ and under a radiation-damage-free condition.¹⁶ The spectra were shown with the binding energy (E_B) from the E_F^S . Purity better than 6N5 for the N₂ did not affect the results.

Figure 1 shows He I_α UPS spectra of the 7-nm-thick CuPc film for the upper valence bands, the VL and the

^{a)}Electronic mail: sueyoshitomoki19@graduate.chiba-u.jp.

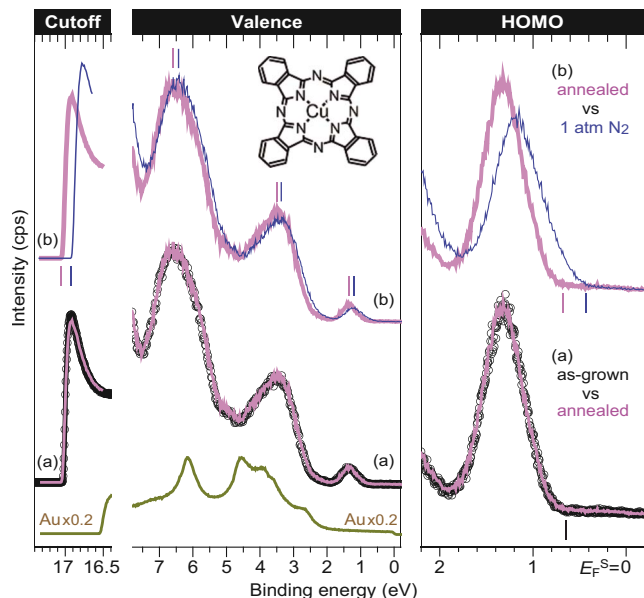


FIG. 1. (Color online) He I_{α} UPS spectra of CuPc(7 nm)/Au at 300 K for as-grown (○), annealed (thick curve) and 1 atm N_2 exposed (thin curve) film for valence bands and secondary cutoff (left panel) and HOMO (right panel) regions. (a) Comparison of as-grown and preannealed film at 343 K for 12 h (before 1 atm N_2 exposure). (b) Comparison of preannealed (before 1 atm N_2 exposure) and 1 atm N_2 exposed film at 300 K for 19 h.

HOMO band regions, where the spectra of the as-grown and preannealed films (a), and the spectra of the N_2 -exposed and preannealed films (b) are compared. The as-grown and preannealed films show similar UPS spectra both in band shape, E_B position, and VL. After the N_2 exposure, in the figure we observe that the HOMO peak shifts to the low E_B side by 0.14 eV and the VL increases by 0.13 eV. There are also remarkable changes both in the HOMO-band width and shape coupled with large HOMO-band tailing into the band gap. Furthermore, the intensity of secondary electrons increases for the N_2 -exposed film. No meaningful change in the spectra was observed for films exposed to low-pressure N_2 ($\sim 5 \times 10^{-3}$ Pa for 12 min). Interestingly, the spectrum almost recovers to the initial one through subsequent postannealing as demonstrated in the following.

Figure 2 compares expanded spectra of the HOMO and band gap regions of the annealed (without N_2 exposure) (a), N_2 -exposed (b), and postannealed (c) films on log intensity scale (panel A). It also compares spectra after subtraction of background signals by the previously reported method⁸ (panel B: see captions) with Gaussian convoluted HOMO bands (solid curves). In Fig. 2, the Fermi-cutoff due to photoemission from the Au substrate is clearly observed for the annealed films (a) (before the N_2 exposure) owing to the ultrahigh detection sensitivity, disappears due to N_2 exposure (b), and appears again due to annealing (c). The spectrum with the N_2 exposure has an exponential-like DOGS that reaches the E_F^S [see panel B(b)]. As seen in panel B, the HOMO band consists of two Gaussian components with different widths for both the annealed and N_2 -exposed films, and these components become much broader upon the N_2 exposure. Consequently, there are three pronounced changes observed in the N_2 -exposed film: (i) the HOMO becomes much broader to give an enhanced Gaussian tailing of the HOMO (Gaussian-type DOGS, parabolic shape on log intensity scale), (ii) an exponential-like DOGS (straight-line-like shape on the log intensity scale) appears near the E_F^S , and (iii) the HOMO shifts to the E_F^S as usually seen after p -type doping. The results demonstrate that gap states, which may originate from the HOMO in imperfect molecular packing, exist near the HOMO onset (the lower E_B side) with a Gaussian shape and further distribute exponentially up to the E_F^S . These DOGSs may control the position of the Fermi level in the film relative to the HOMO band. Such exponential-like DOGSs as well as Gaussian-type DOGSs were also observed for pentacene ultrathin films, where the two types of DOGSs were ascribed to imperfect molecular packing at the interface.⁸ Note that these DOGSs appeared after the N_2 exposure and disappeared after the annealing, although the Gaussian DOGS was not annealed away completely under the present annealing condition. All of these phenomena were observed for repeated N_2 exposure/annealing cycles. Consequently, the results can be ascribed to weak disordering of the CuPc packing structure upon the N_2 exposure that is annealed away by heating. The change in the

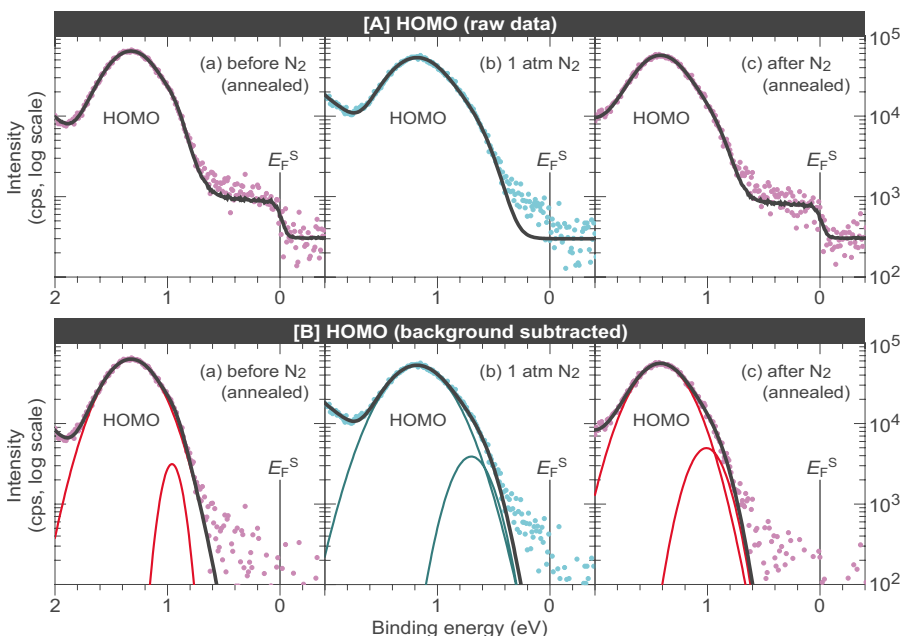


FIG. 2. (Color online) He I_{α} UPS spectra (300 K) of HOMO and band gap region of CuPc(7 nm)/Au on log intensity scale for (a) annealed film at 343 K for 12 h before 1 atm N_2 exposure, (b) 1 atm N_2 exposed film at 300 K for 19 h, and (c) annealed film at 343 K for 15 h after (b). Panel A: Raw UPS spectra (dots) with convoluted curves (black curves) with two Gaussian functions for HOMO (see panel B), photoelectrons from Au substrate and constant background. Panel B: UPS spectra after subtraction of substrate photoelectrons and constant background after intensity normalization of substrate signal at E_F^S (see Ref. 8 for normalization method). Photoelectron intensity from substrate is very small in spectra (b). Convoluted HOMO spectra with two Gaussian functions (parabolas in each spectrum) are also shown by black curves.

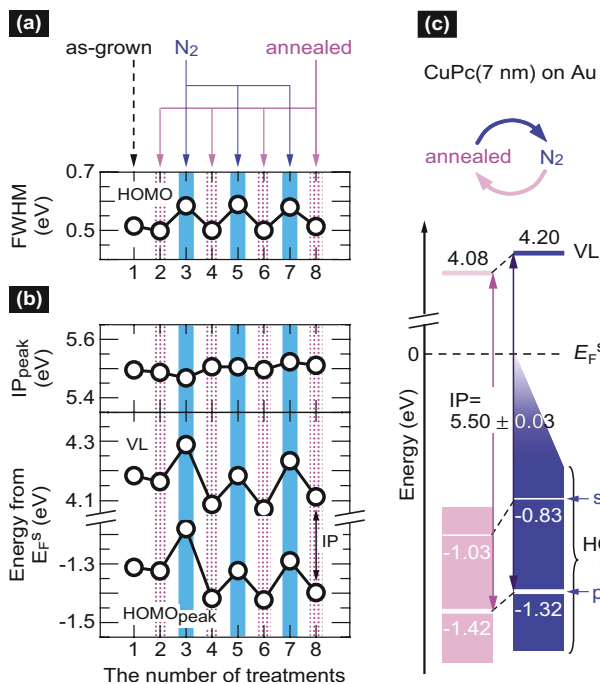


FIG. 3. (Color online) Variations in (a) full width at half maximum of HOMO and (b) ionization potential of HOMO peak (IP_{peak}) and vacuum level (VL) of CuPc(7 nm)/Au after each treatment. Treatment no. 1 corresponds to as-grown film on 300-K substrate; no. 2, no. 4, no. 6, and no. 8 to annealed film at 343 K for 12, 15, 34, and 21 h, respectively; no. 3, no. 5, and no. 7 to 1 atm N_2 exposed film at 300 K for 19 h. (c) Schematic energy diagram of CuPc(7 nm)/Au before and after 1 atm N_2 exposure, with energies after treatments of no. 4 and no. 5. E_B positions of HOMO peak (peak) and shoulder (s) [second Gaussian component, see Fig. 2 (panel B)] are indicated in (c).

Fermi cutoff can also be explained by this disorder mechanism since disordering in the packing structure results in a decrease in the mean-free-path of photoelectrons from the substrate. Note that we have not detected any evidence by UPS that N_2 molecules still exist in the film to give DOGSs after introducing the N_2 -exposed film into the UHV measurement chamber.

Unlike for the present CuPc film on the Au substrate, we could not observe a reversible change in the HOMO-band width and shape in a 7-nm-thick CuPc film prepared on a clean Au(111) surface upon 1 atm air exposure (not shown). This result suggests that the stability of the molecular packing structure in 1 atm gas may be controlled by tuning the properties of the substrate surface. The formation of a well-ordered organic interface would be crucial for producing stable organic devices with the desired properties.

Figure 3 summarizes the values of (a) the full width at half maximum of the HOMO ($FWHM^{\text{HOMO}}$), (b) the E_B (E_B^{HOMO}) and the ionization potential (IP_{peak}) of the HOMO peak and the VL, and (c) energy levels of the N_2 -exposed and annealed films. The CuPc film clearly showed reversible changes upon N_2 exposure/annealing cycles in the E_B^{HOMO} (and the E_B s of other valence bands), the $FWHM^{\text{HOMO}}$, the VL, and the two types of DOGSs, which would be key evidence explaining the ELA and p -type charge transport property of CuPc, while the IP_{peak} stayed at an almost constant value (5.50 ± 0.03 eV) independent of the treatments. In passing, the E_B^{HOMO} and the VL did not recover the initial values after the first N_2 exposure/annealing treatment. This

could originate from contamination of the underlying Au surface upon the first N_2 exposure, since the contamination is not removed at ~ 343 -K annealing, as we observed for the VL of an Au substrate.

The lowest unoccupied molecular orbital also gives the unoccupied gap states such as the HOMO. The energy distributions of these gap states are not symmetric^{15,17} because the wave functions have different spatial spreads. Since these disorder-induced nonsymmetric occupied and unoccupied gap states determine the Fermi level in the gap depending on their densities and energy distributions, the present results place greater importance on disorder-originated gap states not only near the film/substrate interface but also in the bulk of the film. Such disorder-originated gap states may also appear through metal deposition,¹⁸ doping with guest molecules to organic films, and gas exposure.

In summary, we observed reversible changes in the UPS HOMO-band position relative to the Fermi level, the bandwidth, and the shape by 1 atm N_2 exposure and subsequent annealing of the CuPc film while the ionization potential of the HOMO peak remained unchanged. Reversible changes in the band gap states, both the exponential-like DOGS and Gaussian tailing, were also observed. These results demonstrate the importance of molecular packing disorder, which is physically induced by diffusion of N_2 into the film, to the ELA and electrical properties of organic devices.

This work was supported by the Global Center-of-Excellence program (G03, Advanced School for Organic Electronics) (MEXT), a Grant-in-Aid for Scientific Research (A, Grant No. 20245039) (JSPS), and a Grant-in-Aid for Young Scientists (A, Grant No. 20656002) (JSPS). T.S. is grateful for a scholarship from The Futaba Electronics Memorial Foundation.

¹H. Ishii, K. Sugiyama, E. Ito, and K. Seki, *Adv. Mater. (Weinheim, Ger.)* **11**, 605 (1999).

²S. Kera, Y. Yabuuchi, H. Yamane, H. Setoyama, K. K. Okudaira, A. Kahn, and N. Ueno, *Phys. Rev. B* **70**, 085304 (2004).

³N. Koch, *ChemPhysChem* **8**, 1438 (2007).

⁴J. X. Tang, C. S. Lee, and S. T. Lee, *J. Appl. Phys.* **101**, 064504 (2007).

⁵H. Fukagawa, S. Kera, T. Kataoka, S. Hosoumi, Y. Watanabe, K. Kudo, and N. Ueno, *Adv. Mater. (Weinheim, Ger.)* **19**, 665 (2007).

⁶J. Hwang, A. Wan, and A. Kahn, *Mater. Sci. Eng. R.* **64**, 1 (2009).

⁷S. Braun, W. R. Salaneck, and M. Fahlman, *Adv. Mater. (Weinheim, Ger.)* **21**, 1450 (2009).

⁸T. Sueyoshi, H. Fukagawa, M. Ono, S. Kera, and N. Ueno, *Appl. Phys. Lett.* **95**, 183303 (2009).

⁹A. George, *J. Appl. Phys.* **44**, 5148 (1973).

¹⁰M. Honda, K. Kanai, K. Komatsu, Y. Ouchi, H. Ishii, and K. Seki, *J. Appl. Phys.* **102**, 103704 (2007).

¹¹A. Oprea, N. Barsan, and U. Weimar, *Sens. Actuators B* **142**, 470 (2009).

¹²T. Nishi, K. Kanai, Y. Ouchi, M. R. Willis, and K. Seki, *Chem. Phys.* **325**, 121 (2006).

¹³C. Kendrick and S. Semancik, *J. Vac. Sci. Technol. A* **16**, 3068 (1998).

¹⁴A. Kondo, H. Noguchi, S. Ohnishi, H. Kajiro, A. Tohdoh, Y. Hattori, W.-C. Xu, H. Tanaka, H. Kanoh, and K. Kaneko, *Nano Lett.* **6**, 2581 (2006).

¹⁵N. Ueno and S. Kera, *Prog. Surf. Sci.* **83**, 490 (2008), and references therein.

¹⁶M. Ono, T. Sueyoshi, Y. Zhang, S. Kera, and N. Ueno, *Mol. Cryst. Liq. Cryst.* **455**, 251 (2006).

¹⁷J. H. Kang, D. da Silva Filho, J.-L. Brédas, and X.-Y. Zhu, *Appl. Phys. Lett.* **86**, 152115 (2005).

¹⁸T. Sawabe, K. Okamura, T. Sueyoshi, T. Miyamoto, K. Kudo, N. Ueno, and M. Nakamura, *Appl. Phys. A: Mater. Sci. Process.* **95**, 225 (2009).